

A G-CSF functionalized scaffold for stem cells seeding: a differentiating device for cardiac purposes

**Cristiano Spadaccio^a, Alberto Rainer^b, Marcella Trombetta^b, Matteo Centola^b, Mario Lusini^a,
Massimo Chello^a, Elvio Covino^a, Federico De Marco^c, Raffaella Coccia^d,
Yoshiya Toyoda^e, Jorge A. Genovese^{a, e, *}**

^a CIR – Area of Cardiovascular Surgery, University Campus Bio-Medico of Rome, Rome, Italy

^b CIR – Tissue Engineering Laboratory, University Campus Bio-Medico of Rome, Rome, Italy

^c Laboratory of Virology, Regina Elena Institute for Cancer Research, Rome, Italy

^d Department of Biochemical Sciences, Sapienza University of Rome, Rome, Italy

^e Cardiac and Molecular Biology Laboratory, Heart, Lung and Esophageal Surgery Institute,
University of Pittsburgh Medical Center, Pittsburgh, PA, USA

Received: November 23, 2009; Accepted: March 31, 2010

Abstract

Myocardial infarction and its consequences represent one of the most demanding challenges in cell therapy and regenerative medicine. Transfer of skeletal myoblasts into decompensated hearts has been performed through intramyocardial injection. However, the achievements of both cardiomyocyte differentiation and precise integration of the injected cells into the myocardial wall, in order to augment synchronized contractility and avoid potentially life-threatening alterations in the electrical conduction of the heart, still remain a major target to be pursued. Recently, granulocytes colony-stimulating factor (G-CSF) fuelled the interest of researchers for its direct effect on cardiomyocytes, inhibiting both apoptosis and remodelling in the failing heart and protecting from ventricular arrhythmias through the up-regulation of connexin 43 (Cx43). We propose a tissue engineering approach concerning the fabrication of an electrospun cardiac graft functionalized with G-CSF, in order to provide the correct signalling sequence to orientate myoblast differentiation and exert important systemic and local effects, positively modulating the infarction microenvironment. Poly-(L-lactide) electrospun scaffolds were seeded with C2C12 murine skeletal myoblast for 48 hrs. Biological assays demonstrated the induction of Cx43 expression along with morphostructural changes resulting in cell elongation and appearance of cellular junctions resembling the usual cardiomyocyte arrangement at the ultrastructural level. The possibility of fabricating extracellular matrix-mimicking scaffolds able to promote myoblast pre-commitment towards myocardiocyte lineage and mitigate the hazardous environment of the damaged myocardium represents an interesting strategy in cardiac tissue engineering.

Keywords: tissue engineering • 3D scaffold • cardiac graft • electrospinning • PLLA • G-CSF release • connexin 43 • stem cells • differentiation

Introduction

In the general economy of a myocardial infarction, the loss of cardiac tissue triggers a regulated signalling cascade leading to

replacement with scar tissue [1, 2]. The inflammatory state associated with the early phases of wound healing is characterized by a high regenerative and proliferative capacity of both cardiac and mobilized stem cells. These initial adaptive mechanisms, especially sustained by neurohormonal activation, further lead to a deleterious counterpart represented by fibroblasts proliferation and extracellular matrix (ECM) deposition, with the aim to compensate tissue loss and prevent ventricular dilation. At this point, the proliferative capacity and the actual viability of myocardiocytes are dramatically reduced, with the generation of a non-functional scar.

*Correspondence to: Jorge A. GENOVESE, M.D. Ph.D.,
Cardiothoracic Surgery, The University of Utah,
30 N 1900 E, Suite 3C145, Salt Lake City,
UT 84132, USA.
Tel.: 801-587-9294
Fax: 801-585-3936
E-mail: jorge.genovese@utah.edu

This event not only compromises elastic and mechanical properties of the ventricle leading to pump failure, but also is at the root of alterations of the anatomical conduction system, originating potential re-entrant circuits and increasing the risk of ventricular tachyarrhythmias, which represent the main cause for sudden death in heart failure patients [2–4]. In this scenario, stem cell therapy by transfer of bone marrow (BM)-derived stem and precursor cells into the infarcted myocardium has been shown to improve left ventricular systolic function [5]. Similar results were obtained by the application of granulocyte colony-stimulating factor (G-CSF), alone or in combination with stem cell factor, which is known to mobilize BM-derived cells [6–10]. Interestingly, the beneficial effects of these therapies are claimed to be due to a significant degree of structural regeneration of the infarcted hearts by transdifferentiation of the immigrated BM-derived cells to cardiomyocytes [11–15]. However, a true *in situ* cardiac transdifferentiation has not been demonstrated yet, an actual cell viability and engrafting following cell administration have been found to be low, weakening the concept of a real tissue replacement or regeneration [16]. Additionally, new insights on cell-based myocardial repair have been recently reported, shifting emphasis on the importance of paracrine factors secreted by BM-derived cells [17–23]. These findings, together with contradictory results related to the actual transdifferentiation of different cell types used in cardiac therapy [24, 25], raised concerns about an effective, total, functional engraftment of the injected cells. Despite the mechanisms underlying their beneficial effect on cardiac performance, this non-functional integration of injected or endogenously mobilized cells might constitute an arrhythmogenic load within the cardiac environment, increasing the risk for pro-arrhythmia. To this extent, recent reports have shown that the transfer of skeletal myoblasts [26] into decompensated hearts failed to electromechanically integrate and provoked ventricular tachycardias in patients [27]. Moreover, certain types of cardiomyocytes derived from *in vitro* differentiated embryonic stem cells exhibited prolonged action potential durations after depolarizations, and a potential for arrhythmogenesis [28]. The achievement of both a cardiomyocyte differentiation and a precise integration of the injected cells into the myocardial wall, in order to augment synchronized contractility and avoid potentially life-threatening alterations in the electrical conduction of the heart, still remains a major target to be pursued.

Recently, G-CSF fuelled the interest of researchers, not only for its well-known ability to mobilize the endogenous BM-derived stem cells reserve, but also for its direct effect on cardiomyocytes. Harada et al. [9] demonstrated that G-CSF inhibits both apoptosis and remodelling in the failing heart following myocardial infarction through the receptor responsible for cardiac hypertrophy. It has been recently shown that G-CSF activates the Wnt and Jak2 signals in cardiomyocytes, up-regulating connexin 43 (Cx43) protein expression and enhancing its localization on the plasma membrane [29]. Cx43 is a cardiac-specific component of the gap junction complex, recently reported to be involved in modulating arrhythmia and to affect survival following myocardial infarction. Cx43 knockout mice have been shown to exhibit

increased susceptibility to lethal arrhythmia, including ventricular tachycardia and fibrillation, in comparison to wild-type mice [30, 31]. G-CSF treatment suppressed ventricular arrhythmia induced by myocardial infarction, decreased the duration of sustained ventricular tachycardia in *in vivo* settings, and ameliorated survival in a rodent model of myocardial infarction [29]. With this in mind, the therapeutic potential of cell therapy alone needs to be carefully evaluated, especially in light of initial results using skeletal myoblasts that are considered to represent one of the greatest potential myogenic sources for cardiac cell therapy. Intramyocardial injection of these cells failed to consistently show transdifferentiation into cardiomyocytes [32, 33] and, more importantly, electromechanical coupling with the host cardiomyocytes [33–35].

Another major concern in myoblast transplantation, besides the caveat of arrhythmic events, is the loss of a significant fraction of injected myoblasts upon engraftment. A long-term follow-up study of patients suffering from heart failure and treated with myoblast transplantation has shown a consistent reduction in the percentage of cells in the grafted segments exhibiting systolic thickening recovery [36]. In this model, efficiency of myoblast transplantation was hampered by a high rate of cell death, which was incompletely compensated by proliferation within the scar [36]. Considering the enhancing effect of G-CSF on angiogenesis [37], macrophage-induced production of matrix metalloproteases (MMPs) that leads to ECM remodelling [38, 39], and proliferation of L6a1 rat myoblasts before differentiation to myotubes [40], Aharinejad and colleagues genetically engineered myoblasts to overexpress G-CSF prior to transfer to the failing heart following myocardial infarction [41]. This was done in order to improve graft survival, proliferation, blood supply within the scar tissue and eventually cardiac function. Interestingly, they reported an improvement in the left ventricular function and an attenuation of myocardial remodelling only in the G-CSF overexpressed group, with no major associated arrhythmias, warranting animal survival and stable cardiac improvement for more than 80 days [41].

Therefore, new approaches for cell therapy of heart failure should not only improve haemodynamic function, but also aim at a reduction of the vulnerability to arrhythmias. Additionally, a recent report demonstrated that the simple intramyocardial injection of myoblasts results in alterations of myocardium contractile properties at the cellular level, even if without deleterious effects on the global heart function [42].

An alternative approach to cell therapy is represented by tissue engineering, which results from the combination of stem cells and synthetic biodegradable polymers organizing a main frame for cell seeding, survival and proliferation, eventually leading to the production of cell constructs suitable for tissue replacement. In light of the importance of inducing neo-angiogenesis into the inner porosity of the scaffolds, incorporation of angiogenic growth factors such as basic fibroblast growth factor and vascular endothelial growth factor, has been preformed to obtain polymers for controlled release and angiogenesis promotion [43, 44]. Moreover, the relevance of addition of other growth factors and

types of molecular signals to the scaffolds, with the aim to generate a molecular device providing a leading framework for guided cell differentiation and tissue regeneration has been recently pointed out. This concept achieves particular interest in cardiac tissue engineering, where the use of artificial myocardial patches is desirable to limit the geometrical and shape remodeling of the infarcted myocardium and to promote tissue restoration. To this extent, an engineered functionalized myocardium might represent an amenable alternative, as it could provide a mean for mechanical restraint and prevent ventricular dilation. At the same time, it could generate an environment apt to maintain the proliferative capacity of the cells surrounding the infarcted area, providing a molecular pathway to promote cell differentiation [45].

On account of the recent findings regarding a direct effect of G-CSF on cardiomyocyte proliferation and Cx43 expression, we developed a poly(L-lactide) electrospun scaffold releasing G-CSF, and we seeded it with skeletal myoblasts, in order to obtain a tissue engineered cardiac graft. Biological assays demonstrated the induction of Cx43 expression along with morphostructural changes resulting in cell elongation and appearance of cellular junctions resembling the usual cardiomyocyte arrangement at the ultrastructural level. These data, together with other ancillary findings concerning the expression of cardiac-specific isoform of troponin-I, could reliably indicate the ability of this G-CSF functionalized ECM-mimicking scaffold to promote myoblast pre-commitment towards myocardiocyte lineage.

Materials and methods

Scaffold preparation

G-CSF releasing PLLA scaffolds (PLLA/GCSF sample) were prepared by electrospinning, starting from a solution of 13% w/w PLLA (Sigma-Aldrich, Milwaukee, MI, USA) in dichloromethane (Sigma-Aldrich). G-CSF (Filgrastim, 30 MUI/ml, sodium salt, Amgen, Thousand Oaks, CA, USA) was added to the polymer solution at a concentration of 250 UI/g. This concentration was chosen according to both literature and clinical dosage, in order to create a device suitable for direct clinical application [46]. An electrospinning equipment was used (DynaSpin, Biomatica, Rome, Italy); the solution was fed through a 23G needle with a feed rate of 2.5 ml/hr and electrospun onto an earthed collector placed at a distance of 15 cm, using a voltage of 15 kV. Bare PLLA scaffolds (PLLA/Ctrl sample) were also obtained in the same experimental conditions to be used as a control for biological assessments. Microstructure of the obtained membranes was evaluated by field emission scanning electron microscopy (FE-SEM, Leo Supra 1535, Leo Electron Microscopy, Cambridge, UK) coupled to image analysis (ImageTool 3.0, UTHSCSA, San Antonio, TX, USA). Autofluorescence analysis on the polymer was performed in order to assess potential biases or artefacts in further processing for immunostaining. Polymers were excited at different time-points within a range spanning between 10 msec. and 10 sec., and autofluorescence was detected under fluorescence microscope (Olympus, Tokyo, Japan).

Drug release study

Release of G-CSF from the scaffold was assessed by ELISA method, using an instant ELISA kit (Bender MedSystems, Wien, Austria). A total of 0.2 g of PLLA/GCSF scaffold were placed in a sealed tube containing 3 ml of pre-warmed phosphate buffer solution and incubated at 37 °C. A total of 200 µl aliquots were timely collected and assayed according to the manufacturer's instructions.

Mechanical properties

Mechanical properties of the scaffolds were evaluated by longitudinal uniaxial testing using a tensile tester (TH2730, Thumler, Nurnberg, Germany), equipped with a force transducer (Nordisk Transducer Teknik, Hadsund, Denmark). Tests were performed on three PLLA/GCSF patches according to Sell et al. [47]. Briefly, 'dog-bone' shaped segments were measured to obtain length, width and thickness with a dial calliper, connected to the clamps of the tensile tester and loaded at an extension rate of 10 mm/min. Peak stress and strain at failure were calculated starting from load-displacement data collected during the tests as the maximum stress value before failure and its corresponding value of strain, respectively.

Cell seeding

C2C12 mouse skeletal myoblast cell line (ATCC:CRL-1772, passage 4) was used on PLLA/GCSF samples and PLLA/Ctrl controls. Prior to cell culture tests, both PLLA/Ctrl and PLLA/GCSF patches were sterilized by soaking in absolute ethanol (Sigma-Aldrich) [48], punched out to disks 8 mm in diameter and placed into a 96-well plate. A standard static seeding was performed at the density of 500×10^3 cell/cm² as previously described [49]. Briefly, droplets of C2C12 suspension were seeded and incubated overnight. Then 200 µl of the growth medium was added to each well and constructs were cultured for 48 hrs in basal medium (Dulbecco's minimum essential medium – supplemented with 10% fetal bovine serum, 100 units/ml penicillin, 100 µg/ml streptomycin, Lonza, Basel, Switzerland).

At the same time, 2D cell cultures were also performed on 96-well plates, by seeding C2C12 cells at a density of 500×10^3 cell/cm² and culturing them in the same basal medium. After incubation overnight, disks with the diameter of 8 mm of the PLLA/GCSF and PLLA/Ctrl samples (the latter used as control) were added to the culture medium using transwell inserts.

Cell proliferation

Cell proliferation was estimated by total cellular DNA content measurement. Cellular DNA content was obtained as previously described [50]. Briefly, constructs were collected and media removed. Scaffolds were lysed and cells sonicated using a pulse ultrasonic disruptor (Thermo Fisher Scientific, Rockford, IL, USA). DNA content was measured using Quant-iT fluorescence technology (Qubit, Invitrogen, San Diego, CA, USA). Immunostaining for proliferation marker Ki67 was also performed, using rabbit anti-Ki67 primary antibody (Neomarkers, Fremont, CA, USA) and Alexa Fluor 546-conjugated secondary anti-rabbit IgG (Invitrogen).

Cell engraftment and biological assessment

Cell viability, toxicity, attachment, proliferation and differentiation within the scaffolds were evaluated by means immunohistology and confocal microscopy. For cell viability assessment, live/dead assay (Invitrogen) based on cellular membrane intactness was used. The percentage of death and unviable cells was calculated by counting 200 cells in five randomly chosen microscopic fields at 10 \times magnification. Upon culturing, scaffolds were fixed with paraformaldehyde, embedded in Optimal Cutting Temperature (O.C.T.) compound, snap frozen, and cut in 15 μ m slices. Slides were further processed for haematoxylin–eosin staining (Sigma-Aldrich) in order to achieve a morphological analysis. Cell attachment and engraftment were evaluated by means of confocal microscopy, staining cells on the scaffolds for F-actin with Rhodamine Phalloidin (Molecular Probes, Invitrogen), using TOTO[®] (Invitrogen) as nuclear counterstain.

Cell commitment assessment

Immunostaining

Expression of Cx43 and cardiac troponin-I (cTnI) were evaluated by immunocytochemistry and immunofluorescence as previously described [51, 52]. Briefly, frozen tissue sections were permeabilized with 0.1% Triton-X 100 (Sigma-Aldrich) in phosphate buffered saline for 10 min. Non-specific binding of antibodies was blocked by incubating the samples for 45 min. with 2% bovine serum albumin. A mouse monoclonal anti-Cx43 antibody at 1:500 titre and a mouse monoclonal anti-cTnI at 1:500 titre (Chemicon, Millipore, Billerica, MA, USA) were used and subsequently revealed with an Alexa Fluor 488-conjugated secondary antimouse IgG (Invitrogen). In negative control experiments, the incubation with primary antibodies was omitted. Cytoplasmic actin was counterstained with Phalloidin Red (Invitrogen) and for nuclear visualization cells were counterstained with TOTO. Samples were then mounted in Prolong antifade medium (Invitrogen) and viewed under confocal microscopy using an Olympus Fluorview F1000 confocal microscope by two independent blinded observers.

Cytofluorimetry

A set of cultured scaffolds and controls was processed for cytofluorimetry. Cells were recovered from the scaffold incubating it with 0.1% trypsin for 5 min. as previously described [51] and characterized by flow cytometry for Cx43 expression. Additionally, in order to evaluate biological effectiveness of compound release, C2C12 cultured on Petri dishes and exposed to the PLLA/GCSF and PLLA/Ctrl scaffolds were evaluated for Cx43 expression. The obtained cells were pelleted and blocked in 1% CytoPerm and Block solution (BD Biosciences, San Jose, CA, USA), stained using primary antibody against Cx43 (Chemicon) as previously described [53] and run through a flow cytometer Accuri C6 (Accuri Cytometers, Ann Arbor, MI, USA). Appropriate gating was performed to determine Cx43 expression, and a minimum of 50,000 events were collected. Acquired data were analysed using CellQuest software (BD BioSciences).

Western blotting

Cells on scaffolds were lysed by addition of 0.5 ml of lysis buffer per gram of scaffold as previously described [52]. Lysis buffer was composed by 10 mM Tris HCl, 150 mM NaCl, 1% Triton X-100, 5 mM ethylenediaminetetraacetic acid, 1% sodium deoxycholate, 0.1% sodium dodecyl sulphate,

1.2% aprotinin, 5 μ M leupeptin, 4 μ M antipain, 1 mM phenylmethylsulfonyl fluoride and 0.1 mM Na₃VO₄ (Sigma-Aldrich). Protein concentration was determined by bicinchoninic acid (BCA) assay. A total protein amount of 25 μ g of the lysates were subjected to 4–20% SDS-PAGE and transferred to 0.20 μ m nitrocellulose P Membranes (Pierce Biotechnology, Rockford, IL, USA) by means of iBlot device (Invitrogen). Membranes were incubated with antimouse Dystrophin, Cx43 and cTnI antibodies (Chemicon) in phosphate buffered saline, 5% dry milk and 0.1% Tween20 (Sigma-Aldrich) followed by horseradish peroxidase–conjugated secondary antibodies antimouse IgG (Zymed Laboratories, South San Francisco, CA, USA). Antigen–antibody complexes were visualized using enhanced chemiluminescent substrate SuperSignal West PicoTrial Kit (Pierce Biotechnology) on radiographic film. Densitometry analysis was performed with Image-Pro Ver. 6.0 (Media Cybernetics, Silver Spring, MD, USA).

Transmission electron microscopy (TEM)

Samples were routinely prepared as previously described [54]. TEM micrographs of the constructs were obtained with a JEM-2010F FasTEM field emission transmission electron microscope (JEOL, Tokyo, Japan) operated at 100 keV.

Statistical analysis

Data from biological investigations were processed using SPSS (Statistical Package for Social Sciences) release 13.0 for Windows (SPSS, Chicago, IL, USA). Data are presented as mean \pm S.D. One-way ANOVA was performed to compare groups with different treatments, followed by pairwise multiple comparisons procedures (Tukey's test, Holm-Sidak method). Significance was at the 0.05/0.01 levels. Assumptions of normality were checked and met. Pearson's product-moment *r* coefficient was calculated to evaluate correlations. Significance was at the 0.05 level.

Student's t-test was used for analysing fibres average diameter, heparin elution profile and mechanical properties, with a significance at 0.05 levels.

Results

Scaffold characterization

FE-SEM characterization of the electrospun materials revealed a homogeneous distribution of porous fibres with an average diameter of 1.30 \pm 0.40 μ m for PLLA/GCSF sample (Fig. 1A, B). This fibre morphology could represent a suitable environment for cell culturing, as closely mimicking the structure of native ECM, and can potentially provide similar support to cell growth and differentiation.

Autofluorescence of the material was assessed to prevent potential biases in further immunofluorescence analyses; polymer showed autofluorescence only after 8 \pm 0.4 sec.

G-CSF release curve showed an initial burst, followed by a sustained release at a much slower rate. Up to 35% of the loaded G-CSF was released at 1 week (Fig. 2).

Figure 3 shows the tensile behaviour of electrospun material. The stress–strain profile showed a bell-shaped curve with a peak

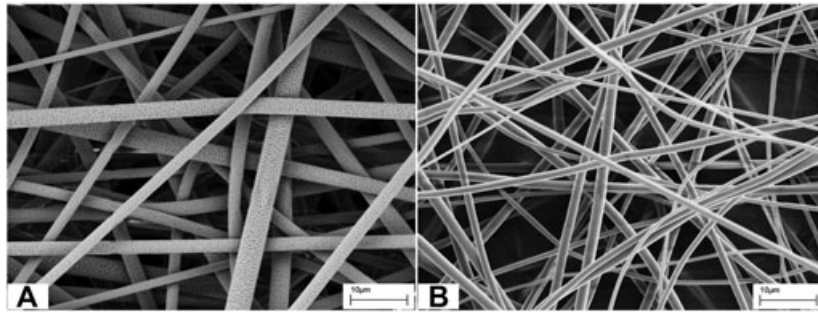


Fig. 1 FE-SEM micrographs of PLLA/Ctrl (A) and PLLA/GCSF (B) electrospun scaffolds.

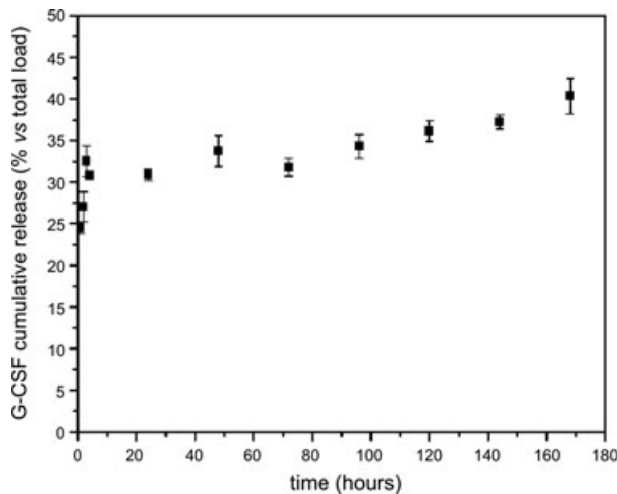


Fig. 2 Drug release curve from PLLA/GCSF scaffold, showing the cumulative release of G-CSF over time.

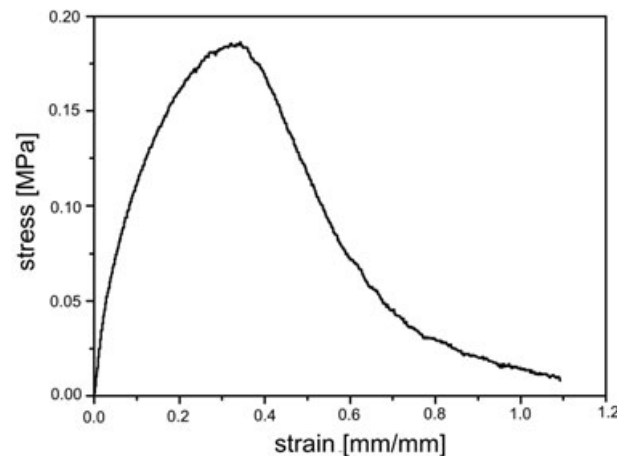


Fig. 3 Stress-strain profile for PLLA/GCSF computed starting from the recorded load-displacement data from longitudinal tensile tests.

stress quantified at 0.188 ± 0.011 MPa and a strain at failure of 0.319 ± 0.016 .

Cell morphology and differentiation

Soon after seeding, high cellularity could be detected in the scaffolds by means of nuclear staining. live/dead assay performed following 48 hrs culture showed a $95 \pm 2\%$ viability, reliably suggesting an effective cell engraftment.

Both light microscopy by means of regular haematoxylin–eosin staining and confocal microscopy by means of cytoplasmic actin and nuclear counterstain, were used to assess cell engrafting and morphology. In PLLA/GCSF sample, C2C12 cells exhibited changes in cell morphology, resulting in a more elongated and spindled cell profile, resembling pole-to-pole cell fusion and fibres rearrangement in striated muscular-like phenotype. Nuclei appeared enlarged, elongated, with loose chromatin and several nucleoli, thus indicating conditions of non-quiescence. In contrast, cells seeded on PLLA/Ctrl scaffold maintained the morphological characteristics they show in conventional culture conditions (Fig. 4A, B).

Cell viability and proliferation, as studied by analysis by live/dead assay, total DNA content per construct and percentage of Ki67+ cells (Fig. 4C–E), demonstrated a statistical significant increase for the cells cultured on PLLA/GCSF scaffolds and for the 2D cell cultures exposed to PLLA/GCSF ($P < 0.001$).

Immunofluorescence analysis revealed Cx43 expression, along with a higher fibrillar distribution of cytoplasmic actin in the PLLA/GCSF scaffolds, with respect to the PLLA/Ctrl control (Fig. 5A–F). Cx43 antibody nicely stained membranes of cells engrafted among polymeric fibres, but could also be detected in the perinuclear zone. Flow cytometry confirmed and quantified Cx43 positivity, showing a statistical significant higher level of expression in the PLLA/GCSF scaffold. Interestingly, a significant increase in Cx43 positivity could be observed in 2D cell cultures exposed to PLLA/GCSF, in comparison with PLLA/Ctrl control (Fig. 6A). Immunofluorescence also showed appearance of cardiac-specific isoform of troponin I in the PLLA/GCSF group. Interestingly, antigen was localized in cytoplasm and presented a granular pattern of expression, clearly indicating a non-mature organization of the protein inside the cell (Fig. 7B). These results were confirmed with Western blotting analysis that showed

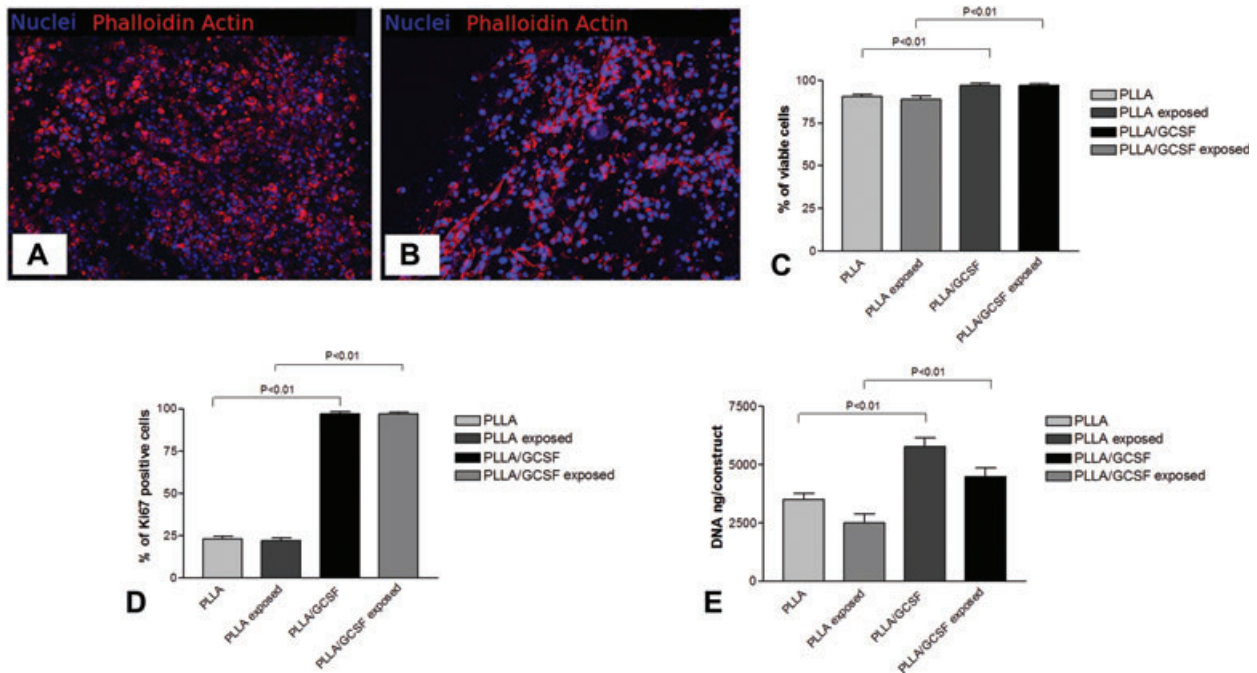


Fig. 4 (A) PLLA/Ctrl seeded with C2C12 after 48 hrs culturing (100 \times); (B) PLLA/GCSF seeded with C2C12 after 48 hrs culturing (100 \times); (C) cells viability analysis in PLLA/GCSF and in PLLA/Ctrl scaffolds after 48 hrs of culture; (D) cell proliferation evaluated by measuring the total DNA content per construct; (E) percentage of Ki67 expression in both types of scaffolds. An increase in cell viability and proliferation could be detected in the PLLA/GCSF scaffold in comparison to PLLA/Ctrl scaffolds.

co-expression of Cx43 and cTnI in the PLLA/GCSF patches, confirming a cardiac pre-commitment of myoblasts seeded in these scaffolds and a direct effect of G-CSF released from the polymer on cells in conventional culture (Fig. 6B). A non-cardiac specific dystrophin antibody recognizing a 60 kD fragment of the native protein was used as a general marker for myoblasts. The contemporary presence of both myoblast and cardiac-specific markers could reliably suggest different stages in the differentiation process. However, morphological and immunophenotypic changes achieved by myoblasts in this setting were not compatible with a complete differentiation in cardiomyocyte and cells did not acquire beating capability which is related to the appearance of a functional cardiac-specific calcium handling system.

Transmission electron microscopy

TEM analysis revealed engrafted myoblasts closely adhering on PLLA fibres. Cells on PLLA/GCSF polymer appeared elongated with more evidently represented rough endoplasmic reticulum (RER) and Golgi apparatus with respect to the control scaffold, reliably indicating a higher metabolic activity (Fig. 8A, B). Elongated eccentric mitochondria, typical of muscular cells, could be detected on releasing scaffold (Fig. 8C). Along with these findings, several types of cellular junctions could be observed (Fig. 8D–F). Kissing junctions among cells on both PLLA/Ctrl and

PLLA/GCSF scaffolds could be detected. However, in the latter, more complex and highly organized intercellular structures could be observed. Figure 8F shows a particular of a cell-to-cell junction characterized by a suggestive three-layered electron-dense complex, with the layers constituting the structure being highly rugous. Together with the detection of Cx43⁺ cells and the perimembraneous distribution of this antigen, the findings described at TEM analysis could reliably suggest the presence of gap junctions. The presence of cytoplasmic vesicles and of a highly represented RER and Golgi apparatus in the PLLA/GCSF scaffold, could allow speculation of an active production of Cx43 as an early step of membranous gap junction formation.

Discussion

Cell therapy for the globally ischemic heart has been investigated during the past decade. The first clinical trials were performed by Menasche et al. using autologous skeletal myoblasts [27] with encouraging results concerning increases in regional wall motion and in left ventricular ejection fraction. Myoblasts are resistant to ischaemia, and showed ability to improve ventricular function in animal models [32], differentiating into myotubes *in vivo*. Unfortunately, a true cardiomyocytic phenotype could not be

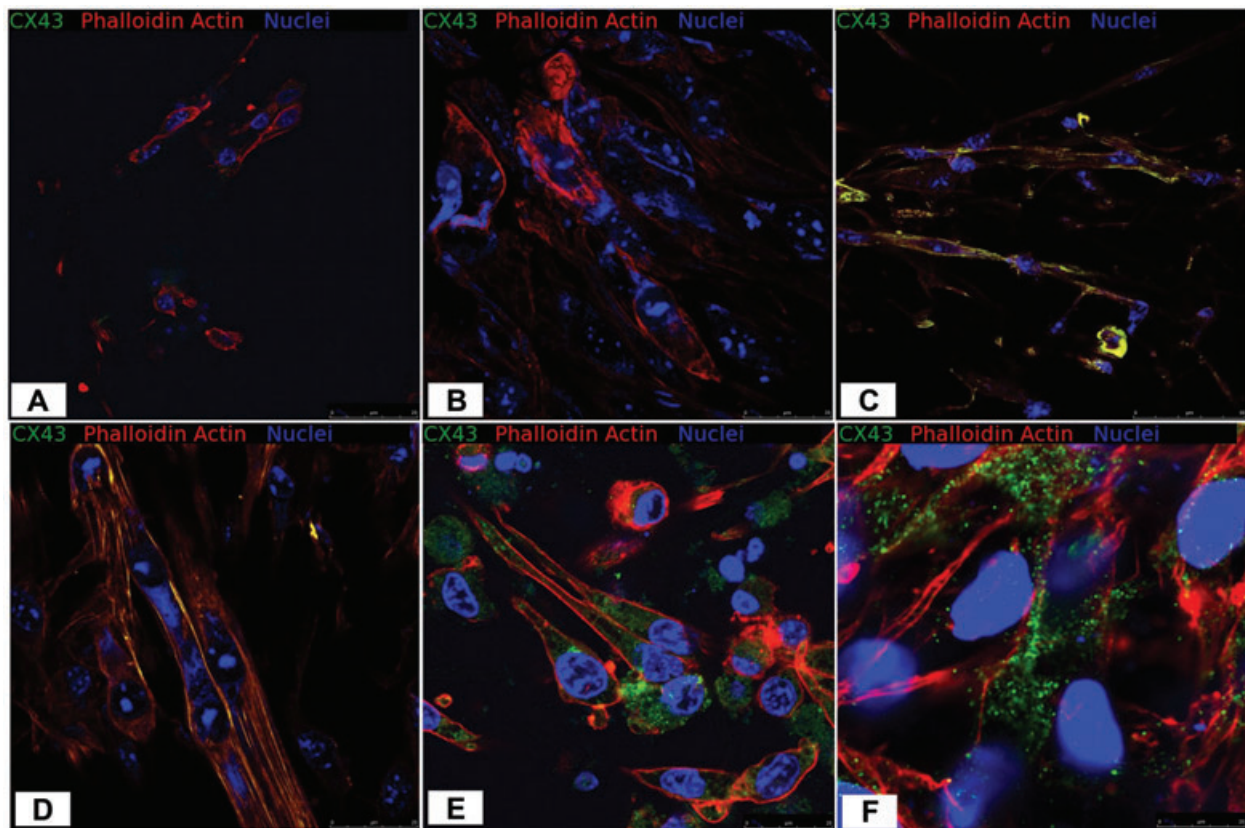


Fig. 5 Confocal microscopy. Immunofluorescence staining for Cx43, F-actin and nuclei. (A, B) PLLA/Ctrl seeded with C2C12 after 48 hrs (400 \times). (C–F) PLLA/GCSF seeded with C2C12 after 48 hrs (400 \times). Cx43 expression and a higher fibrillar distribution of cytoplasmic actin in the PLLA/GCSF scaffolds, with respect to the PLLA/Ctrl control could be seen (A–F). Cx43 antibody nicely stained membranes of cells (C, D, F) engrafted among polymeric fibres, but could also be detected in the perinuclear zone (E).

achieved in several experimental efforts [55], and myotubes do not integrate electrically with surviving cardiomyocytes [55], failing to contract synchronously with the surrounding myocardium. However, the increased recognition that other types of adult stem cells have a much more limited plasticity than initially promised [56], together with the contradictory results related to the actual transdifferentiation of different cell types used in cardiac therapy [24, 25], allow considering a cell type already committed towards muscle phenotype, closely reminding cardiac cytoarchitecture, as a still valid alternative for cell therapy. Therefore, the idea to overcome myoblasts current limitations, leading to an 'optimized' use of this cell type, remains attractive and feasible [56]. Aharinejad and colleagues engineered myoblast to overexpress G-CSF improving local angiogenesis following injection and therefore graft survival, proliferation, blood supply within the scar tissue and eventually overall cardiac function [41].

However, the usual direct injection delivery modality is hampered by several limitations that may minimize effectiveness of the procedure. Pro-inflammatory state related to needle-induced tissue laceration with embolization phenomena, induced apoptosis due to detachment of anchorage-dependent cells from their ECM,

and ischaemia related to grafting cells deprived from their own vascular supply in poorly perfused target areas are considered main pitfalls of this technique [56]. Moreover, both the interventional procedure and the non-functional integration of injected cells in the myocardial host environment have been shown to potentially lead to life-threatening arrhythmias.

One possible approach to overcome these hurdles could be to use biodegradable scaffolds seeded with the candidate cell to reproduce the ECM structure and topography, with the aim to produce a biological surrogate as close as possible to the native histoarchitecture and able to support and guide cell attachment and proliferation. Siepe *et al.* recently used a highly porous myoblast-seeded polyurethane scaffolds demonstrating their ability to prevent post-myocardial infarction progression towards heart failure in a rat model with no evidence of transdifferentiation of the seeded myoblasts towards cardiac cells or migration from the scaffold to the heart [57, 58].

To date, several types of polymers have been proposed to obtain cardiac grafts and PLLA polymers represent the most attractive avenues for this purpose because of their advantageous mechanical properties, plasticity and biocompatibility [59]. Many

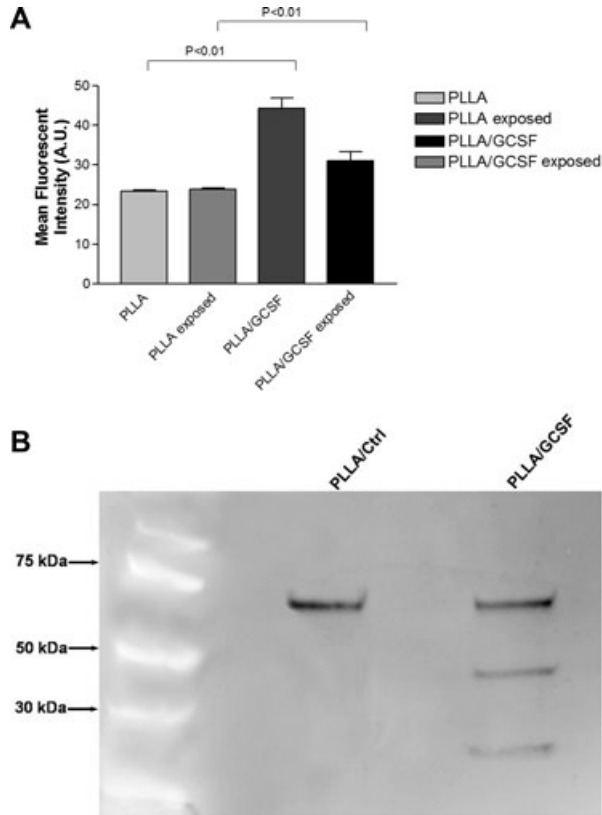


Fig. 6 (A) Cytofluorimetry analysis of Cx43 expression. **(B)** Western Blot for dystrophin, Cx43 and cTnI; MW: molecular weight marker. Lane 1: PLLA/Ctrl seeded with C2C12 for 48 hrs; lane 2: PLLA/GCSF scaffold seeded with C2C12 for 48 hrs. A non-cardiac specific dystrophin antibody recognizing a 60 kD fragment of the native protein was used as a general marker for myoblasts. The contemporary presence of both myoblast and cardiac-specific markers could reliably suggest different stages in the differentiation process.

different techniques have been developed for the construction of cardiovascular scaffolds with this polymer. Electrospinning is one of the most effective and functional approaches [60], with the possibility of being combined to the newest methodologies of cell seeding [61, 62]. The electrospinning process allows for control over the morphology of the fibres and use of a wide variety of polymers. The small diameter fibres produced by electrospinning have the advantage of a large surface-to-volume ratio, as well as a high permeability and interconnecting pore structure, both of which are desirable in a biological setting.

Also, polymers combined with grow factors, cytokines and drugs have been developed [48, 63], generating drug releasing systems capable of focused and localized delivery of molecules according to the local environment requirements. A broad range of applications for electrospun fibres has been suggested [64, 65], ranging from drug delivery [66–70] to gene therapy [71]. A large variety of biopolymeric scaffolds has been functionalized with

growth factors, to act as drug delivery systems. More interestingly, the potential of such ECM-mimicking systems could be oriented to obtain a leading framework providing adequate signalling for engraftment, proliferation, and differentiation of stem or pre-committed cells towards different phenotypes.

Recently, our group has developed a hydroxyapatite functionalized electrospun PLLA scaffold with the aim of recapitulating the native histoarchitecture and the molecular signalling of osteochondral tissue to facilitate cell differentiation towards chondrocyte. PLLA/hydroxyapatite nanocomposites induced differentiation of hMSCs in a chondrocyte-like phenotype with generation of a proteoglycan-based matrix [72]. Moreover, we produced some preliminary data on scaffold tailored for cardiovascular structures [73]. These data represent a proof of principle of the possibility to produce a scaffold suitable for stem cells seeding, containing the appropriate factors to induce a guided differentiation towards the desired phenotype. In these settings differentiation would be realized within a 3D ECM-like environment closely mimicking the tissue native architecture and allowing a harmonious ongoing cell growth and differentiation for tissue regeneration.

Recent studies indicate that there is a lack of functional electromechanical coupling between the majority of grafted myoblasts and cardiomyocytes [34, 35]. G-CSF has been shown to induce the expression of Cx43 [29], a cardiac-specific gap junction protein crucial for effective electromechanical association [30, 31]. The idea to produce a biodegradable device able to induce differentiation of myoblasts – one of the most commonly used cell types in cardiac therapy – in order to ameliorate their engrafting and effectiveness, guided us to explore the potential role of a G-CSF functionalized PLLA scaffold for myocardial tissue engineering. To our knowledge, the association of electrospun poly(lactide) polymer and G-CSF for cardiovascular differentiation purposes is novel.

For drug loading, a direct incorporation of the growth factor during the scaffold preparation has been performed as previously described [74]. In contrast with adsorption or microencapsulation, this approach overcomes the drawbacks of these methods [75] and allows mild solvent use and low processing temperature preserving molecules bioactivity and providing a sustained release. Scaffold was characterized as composed of a non-woven mesh of randomly oriented, micron-sized fibres. This morphology could provide a favourable environment to cell attachment, growth and differentiation as closely mimicking the structure of native ECM recapitulating the arrangement of connective tissue fibrillar proteins. These intrinsic properties have been shown to allow the remodelling of vascular grafts in both the cellular and ECM content thus representing an optimal candidate for tissue-engineered cardiac graft fabrication [76]. Release profile of the growth factor was also evaluated, indicating a burst release occurring in the first hours, attributable to the elution of the excess drug on the surface of the scaffold, followed by a slower release rate.

Mechanical behaviour of electrospun material, evaluated by tensile testing, was found to be compatible with the model of a fibrillar material, exhibiting a progressive failure of fibre elements for high stress values, and resulting in a bell-shaped stress–strain

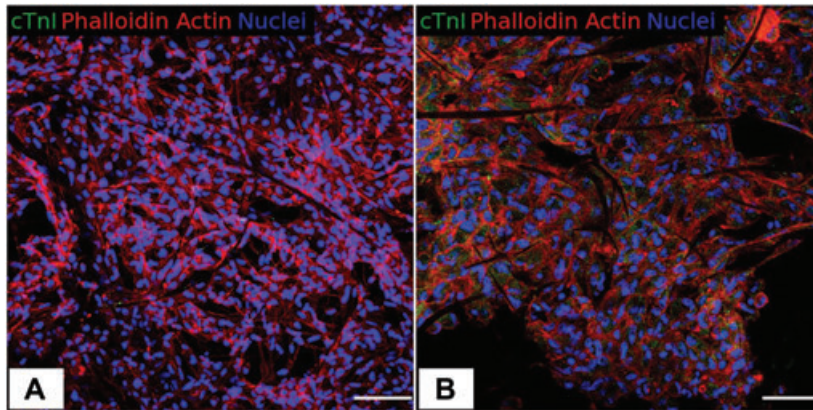


Fig. 7 Confocal microscopy. Immunofluorescence staining for cTnI, F-actin and nuclei. **(A)** PLLA/Ctrl seeded with C2C12 after 48 hrs (400 \times). **(B)** PLLA/GCSF seeded with C2C12 after 48 hrs (400 \times). cTnI expression was found only in the PLLA/GCSF sample, with a cytoplasmatic and granular pattern of expression, that indicates a non-mature organization of the protein inside the cells. Scale bar: 100 μ m.

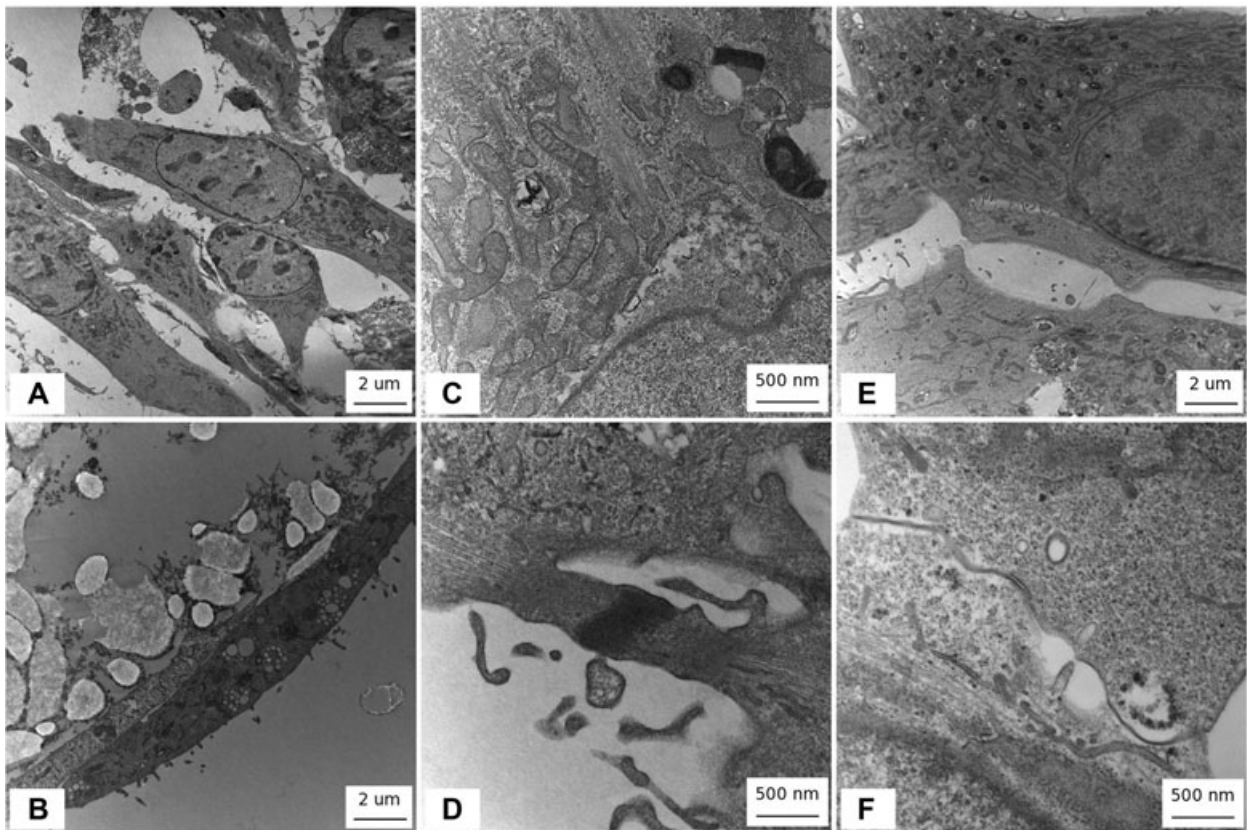


Fig. 8 TEM. **(A, E)** PLLA/Ctrl **(B, C, D, F)** PLLA/GCSF. Note cells on PLLA-GCSF polymer appeared elongated with more evidently represented RER and Golgi apparatus with respect to non-functionalized scaffolds **(A–B)**, reliably indicating a higher metabolic activity. Elongated eccentric mitochondria typical of muscular cells could be detected on functionalized scaffolds **(C)**. In the functionalized scaffold, several types of cell-to-cell interactions could be observed with cells acquiring a typical fuse-shape phenotype with elongated nuclei. Alignment of cells resembling myotube organization could be observed and electrondense fibrillar structures in the contact zone between cells could be seen **(D)**. Membrane-to-membrane contact could be detected among cells seeded on bare PLLA scaffolds. In the functionalized scaffold a particular of a cell-to-cell junction characterized by a suggestive three-layered electron dense complex could be observed. Layers constituting the structure appeared highly rugous **(E–F)**.

curve. The obtained values for the strain at failure of PLLA/GCSF constructs were found compatible to the values for myocardial tissue reported in the literature [77–79]. Scaffolds were seeded with C2C12 and evaluated in terms of cell engraftment, viability, proliferation and differentiation. Light and confocal microscopy was consistent with an adequate cell attachment and viability, with cells cultured in the drug-loaded scaffolds exhibiting morphostructural changes resulting in cell elongation, spindled cell profile, images of pole-to-pole cell fusion and rearrangement of fibres in striated muscular-like phenotype. Proliferation analysis, together with the immunofluorescence staining revealing the presence of Ki67+ cells, confirmed the generation of a non-hostile microenvironment for cell culturing, with an additional proliferative drive reliably induced by the scaffold. Some of the reasons for PLLA being widely used in the medical field include its biocompatibility, mechanical properties and biodegradability. PLLA degrades by hydrolysis, and its degradation products can be metabolized. PLLA degrades to lactic acid *via* hydrolytic de-esterification, and lactic acid forms pyruvate by lactate dehydrogenase. Pyruvate is an intermediate product in metabolic pathways, and it can generate glucose *via* gluconeogenesis or be metabolized to form CO₂ and water by the citric acid cycle [80]. Therefore, PLLA hydrolysis is not supposed to exert significant toxic effects *in vitro* and *in vivo* settings. In the present study, 2D cell cultures were also performed to evaluate the effect of scaffold by-products on cell viability and toxicity as well as differentiation. These experiments in two dimensions, along with similar analysis in 3D cultures, showed no significant changes or impairments in cell viability or survival, confirming the generation of a non-hostile environment and allowing to reliably discard a negative effect of the PLLA on cells or tissues. Additionally, especially in the functionalized scaffold, we could demonstrate that exposure to eluted drug could exert functional effects on C2C12 in terms of differentiation, thus confirming functional integrity of G-CSF molecule.

A shift towards Cx43 positivity could be detected in the functionalized polymers with respect to the PLLA/Ctrl control, thus indicating a possible cardiac commitment, associated to the stimuli contained in the scaffold. Ultrastructural analysis by TEM showed suggestive three-layered electron dense complexes with the layers constituting the structures being highly rugous. These structures could not be observed in the control scaffold in which cell-to-cell interaction remained at the level of a simple contact apparently without any further degree of structural organization. Taken together, the detection of Cx43 with its perimembraneous distribution and the morphological and ultrastructural changes described at TEM analysis, allow us to reliably speculate about the formation of gap junctions-like structures probably driven by the presence of G-CSF. This hypothesis is reinforced by the previous demonstration of the effect of G-CSF on the expression of Cx43, a cardiac-specific gap junction protein [29]. The presence, in cells cultured on PLLA/GCSF scaffolds, of cytoplasmic vesicles and highly represented RER and Golgi apparatus, together with the detection at immunofluorescence of Cx43 in both perimembraneous and perinuclear location, could allow speculating an active production of Cx43 as an early step of membranous gap junction

formation. To confirm myocardial pre-commitment, expression of another cardiac-specific marker, c-TnI, was evaluated. Immunofluorescence showed appearance of cardiac-specific isoform of troponin I in the PLLA/GCSF group. Antigen was localized in cytoplasm and presented a granular pattern of expression, clearly indicating a non-mature organization of the protein inside the cell.

G-CSF was found to improve angiogenesis following myoblast injection in a cardiac ischaemic model [81]. The capacity of myoblasts transplants to regenerate myocardial tissue following infarction depends on nourishment and spatially appropriate growth of myoblasts. This requires a potent neovasculature, appropriate MMP activity and proper fibrillar collagen scaffolding. As shown by cell transfection with G-CSF, this growth factor can enhance the number of grafted myoblasts mainly in relation to the increased induced angiogenesis [41]. Consistent with these angiogenic effects, G-CSF has been shown to stimulate monocytes, progenitors of macrophages, to secrete vascular endothelial growth factor and regulate angiogenesis [39]. Moreover, G-CSF has been shown to positively influence ventricular remodelling through promotion of reparative collagen synthesis (types I and III) in the infarcted area [10]. Considering the action of ventricular restraint claimed to be at the root of the success of some cardiac tissue engineering approaches, the possibility to modulate collagen production through the implantation of this PLLA/GCSF scaffold would be attractive, and will be subject of further investigation.

In this study we demonstrated the ability of a 3D ECM-mimicking scaffold releasing G-CSF to induce a cardiac pre-commitment of skeletal myoblasts. C2C12 achieved an only partial cardiomyocyte-like phenotype expressing cardiac-specific Cx43 and troponin-I, potentially useful to facilitate functional integration with cardiomyocytes. Morphological and immunophenotypic changes achieved by myoblasts in this setting were not compatible with a complete differentiation in cardiomyocyte and cells did not acquire beating capabilities, subordinated to the appearance of cardiac-specific calcium handling systems. However, the final scope of the work consisted in the possibility to generate a suitable tissue-engineered graft able to overcome current limitations of cardiac patches and myoblast cell therapy, which mainly concern non-functional electromechanical integration within the host myocardium. Therefore, our final aim was not the achievement of a total differentiated phenotype. In light of an *in vivo* application, a fully differentiated beating phenotype could paradoxically fail to integrate with the host because of asynchronous beating activity and potentially constitute an arrhythmogenic focus leading to life threatening arrhythmias. On the contrary, our interest was to optimize the myoblast phenotype within a 3D environment to generate a more performing cardiac graft able to overcome the current limitations of cardiac cell therapy [56]. As we have previously reported, inducing a partial differentiation towards a cardiac pre-committed phenotype, expressing some of the key proteins of a mature cardiomyocyte, could represent an interesting strategy to provide a better integration within the cardiac environment. The pre-differentiated cells would receive signals from the new environment, thus achieving a gradual ongoing complete differentiation

[16]. Additionally, combination of stem cells or pre-differentiated stem cells with biomaterials organized in 3D structured matrices reproducing the ECM, could represent an alternative strategy to obtain a full tissue restoration and to prevent ventricular remodeling. To this extent, biocompatible materials could be further functionalized with different growth factors in order to guide tissue regeneration and to promote *in situ* completion of differentiation of pre-committed progenitor cells [16].

Conclusion

The concept of synthesizing a scaffold containing factors, able at the same time to orientate stem cell differentiation and exert important systemic and local effects, positively modulating the infarction microenvironment, could represent an attractive alternative to the currently used approach in cardiac tissue engineering. On account of the more demanding needs of the emerging branches of reconstructive medicine, we proposed the fabrication of scaffolds providing the correct sequences of signals to both promote cell adhesion, pre-commitment and matrix remodelling.

References

1. Frangogiannis NG. Chemokines in the ischemic myocardium: from inflammation to fibrosis. *Inflamm Res.* 2004; 53: 585–95.
2. Chamberlain DA. Overview of completed sudden death trials: European experience. *Cardiology.* 1987; 74: 10–23.
3. Demirovic J, Myerburg RJ. Epidemiology of sudden coronary death: an overview. *Prog Cardiovasc Dis.* 1994; 37: 39–48.
4. Myerburg RJ, Kessler KM, Castellanos A. Sudden cardiac death. Structure, function, and time-dependence of risk. *Circulation.* 1992; 85: 12–10.
5. Drexler H, Meyer GP, Wollert KC. Bone-marrow-derived cell transfer after ST-elevation myocardial infarction: lessons from the BOOST trial. *Nat Clin Pract Cardiovasc Med.* 2006; 3: S65–8.
6. Kang HJ, Kim HS, Koo BK, et al. Intracoronary infusion of the mobilized peripheral blood stem cell by G-CSF is better than mobilization alone by G-CSF for improvement of cardiac function and remodeling: 2-year follow-up results of the Myocardial Regeneration and Angiogenesis in Myocardial Infarction with G-CSF and Intra-Coronary Stem Cell Infusion (MAGIC Cell) 1 trial. *Am Heart J.* 2007; 153: 237 e1–8.
7. Kang HJ, Kim HS, Zhang SY, et al. Effects of intracoronary infusion of peripheral blood stem-cells mobilised with granulocyte-colony stimulating factor on left ventricular systolic function and restenosis after coronary stenting in myocardial infarction: the MAGIC cell randomised clinical trial. *Lancet.* 2004; 363: 751–6.
8. Kang HJ, Lee HY, Na SH, et al. Differential effect of intracoronary infusion of mobilized peripheral blood stem cells by granulocyte colony-stimulating factor on left ventricular function and remodeling in patients with acute myocardial infarction versus old myocardial infarction: the MAGIC Cell-3-DES randomized, controlled trial. *Circulation.* 2006; 114: 1145–51.
9. Harada M, Qin Y, Takano H, et al. G-CSF prevents cardiac remodeling after myocardial infarction by activating the Jak-Stat pathway in cardiomyocytes. *Nat Med.* 2005; 11: 305–11.
10. Sugano Y, Anzai T, Yoshikawa T, et al. Granulocyte colony-stimulating factor attenuates early ventricular expansion after experimental myocardial infarction. *Cardiovasc Res.* 2005; 65: 446–56.
11. Orlic D. Adult bone marrow stem cells regenerate myocardium in ischemic heart disease. *Ann N Y Acad Sci.* 2003; 996: 152–7.
12. Orlic D, Kajstura J, Chimenti S, et al. Transplanted adult bone marrow cells repair myocardial infarcts in mice. *Ann N Y Acad Sci.* 2001; 938: 221–9; discussion 9–30.
13. Orlic D, Kajstura J, Chimenti S, et al. Bone marrow stem cells regenerate infarcted myocardium. *Pediatr Transplant.* 2003; 7: 86–8.
14. Orlic D, Kajstura J, Chimenti S, et al. Bone marrow cells regenerate infarcted myocardium. *Nature.* 2001; 410: 701–5.
15. Orlic D, Kajstura J, Chimenti S, et al. Mobilized bone marrow cells repair the infarcted heart, improving function and survival. *Proc Natl Acad Sci USA.* 2001; 98: 10344–9.
16. Spadaccio C, Chachques E, Chello M, et al. Predifferentiated Adult Stem Cells and Matrices for Cardiac Cell Therapy. *Asian Cardiovasc Thorac Ann.* 2009; 17: 1–9.
17. Gneccchi M, He H, Liang OD, et al. Paracrine action accounts for marked protection of ischemic heart by Akt-modified mesenchymal stem cells. *Nat Med.* 2005; 11: 367–8.
18. Gneccchi M, He H, Noiseux N, et al. Evidence supporting paracrine hypothesis

Our aim was to reproduce a microenvironment able not only to assist and guide cell growth, differentiation and repopulation, but also to mimic the mechanical properties of the native connective tissue and to receive important signaling once within the organism. In addition, the localized controlled growth factor delivery, minimizing the undesired systemic effects, could lead to a powerful device for wound repair in the *in vivo* setting, allowing a coordinated healing response, respecting and finely modulating wound site and tissue homeostasis.

Acknowledgements

These studies were partially supported by the University of Pittsburgh Medical Center Heart, Lung & Esophageal Surgery Institute. The authors are thankful to Dr. Franca Abbruzzese for her valuable help.

Conflict of interest

The authors confirm that there are no conflicts of interest.

- for Akt-modified mesenchymal stem cell-mediated cardiac protection and functional improvement. *FASEB J.* 2006; 20: 661–9.
19. **Mirotsov M, Zhang Z, Deb A, et al.** Secreted frizzled related protein 2 (Sfrp2) is the key Akt-mesenchymal stem cell-released paracrine factor mediating myocardial survival and repair. *Proc Natl Acad Sci USA.* 2007; 104: 1643–8.
 20. **Dai W, Hale SL, Kloner RA.** Role of a paracrine action of mesenchymal stem cells in the improvement of left ventricular function after coronary artery occlusion in rats. *Regen Med.* 2007; 2: 63–8.
 21. **Ohnishi S, Sumiyoshi H, Kitamura S, et al.** Mesenchymal stem cells attenuate cardiac fibroblast proliferation and collagen synthesis through paracrine actions. *FEBS Lett.* 2007; 581: 3961–6.
 22. **Mayer H, Bertram H, Lindenmaier W, et al.** Vascular endothelial growth factor (VEGF-A) expression in human mesenchymal stem cells: autocrine and paracrine role on osteoblastic and endothelial differentiation. *J Cell Biochem.* 2005; 95: 827–39.
 23. **Li L, Zhang S, Zhang Y, et al.** Paracrine action mediate the antifibrotic effect of transplanted mesenchymal stem cells in a rat model of global heart failure. *Mol Biol Rep.* 2009; 36: 725–31.
 24. **Murry CE, Soonpaa MH, Reinecke H, et al.** Haematopoietic stem cells do not transdifferentiate into cardiac myocytes in myocardial infarcts. *Nature.* 2004; 428: 664–8.
 25. **Reinecke H, Poppa V, Murry CE.** Skeletal muscle stem cells do not transdifferentiate into cardiomyocytes after cardiac grafting. *J Mol Cell Cardiol.* 2002; 34: 241–9.
 26. **Chachques JC, Herreros J, Trainini J, et al.** Autologous human serum for cell culture avoids the implantation of cardioverter-defibrillators in cellular cardiomyoplasty. *Int J Cardiol.* 2004; 95: S29–33.
 27. **Menasche P, Hagege AA, Vilquin JT, et al.** Autologous skeletal myoblast transplantation for severe postinfarction left ventricular dysfunction. *J Am Coll Cardiol.* 2003; 41: 1078–83.
 28. **He JQ, Ma Y, Lee Y, et al.** Human embryonic stem cells develop into multiple types of cardiac myocytes: action potential characterization. *Circ Res.* 2003; 93: 32–9.
 29. **Kuwabara M, Kakinuma Y, Katare RG, et al.** Granulocyte colony-stimulating factor activates Wnt signal to sustain gap junction function through recruitment of beta-catenin and cadherin. *FEBS Lett.* 2007; 581: 4821–30.
 30. **Lerner DL, Yamada KA, Schuessler RB, et al.** Accelerated onset and increased incidence of ventricular arrhythmias induced by ischemia in Cx43-deficient mice. *Circulation.* 2000; 101: 547–52.
 31. **van Rijen HV, Eckardt D, Degen J, et al.** Slow conduction and enhanced anisotropy increase the propensity for ventricular tachyarrhythmias in adult mice with induced deletion of connexin43. *Circulation.* 2004; 109: 1048–55.
 32. **Menasche P.** Skeletal myoblasts as a therapeutic agent. *Prog Cardiovasc Dis.* 2007; 50: 7–17.
 33. **Murry CE, Field LJ, Menasche P.** Cell-based cardiac repair: reflections at the 10-year point. *Circulation.* 2005; 112: 3174–83.
 34. **Rubart M, Soonpaa MH, Nakajima H, et al.** Spontaneous and evoked intracellular calcium transients in donor-derived myocytes following intracardiac myoblast transplantation. *J Clin Invest.* 2004; 114: 775–83.
 35. **Leobon B, Garcin I, Menasche P, et al.** Myoblasts transplanted into rat infarcted myocardium are functionally isolated from their host. *Proc Natl Acad Sci USA.* 2003; 100: 7808–11.
 36. **Hagege AA, Marolleau JP, Vilquin JT, et al.** Skeletal myoblast transplantation in ischemic heart failure: long-term follow-up of the first phase I cohort of patients. *Circulation.* 2006; 114: 1108–13.
 37. **Aharinejad S, Marks SC Jr, Bock P, et al.** CSF-1 treatment promotes angiogenesis in the metaphysis of osteopetrotic (toothless, *tl*) rats. *Bone.* 1995; 16: 315–24.
 38. **Tojo N, Asakura E, Koyama M, et al.** Effects of macrophage colony-stimulating factor (M-CSF) on protease production from monocyte, macrophage and foam cell *in vitro*: a possible mechanism for anti-atherosclerotic effect of M-CSF. *Biochim Biophys Acta.* 1999; 1452: 275–84.
 39. **Aharinejad S, Abraham D, Paulus P, et al.** Colony-stimulating factor-1 antisense treatment suppresses growth of human tumor xenografts in mice. *Cancer Res.* 2002; 62: 5317–24.
 40. **Borycki AG, Smadja F, Stanley R, et al.** Colony-stimulating factor 1 (CSF-1) is involved in an autocrine growth control of rat myogenic cells. *Exp Cell Res.* 1995; 218: 213–22.
 41. **Aharinejad S, Abraham D, Paulus P, et al.** Colony-stimulating factor-1 transfection of myoblasts improves the repair of failing myocardium following autologous myoblast transplantation. *Cardiovasc Res.* 2008; 79: 395–404.
 42. **Giraud MN, Liechti EF, Tchantchaleishvili V, et al.** Myocardial injection of skeletal myoblasts impairs contractility of host cardiomyocytes. *Int J Cardiol.* 2010; 138: 131–7.
 43. **Perets A, Baruch Y, Weisbuch F, et al.** Enhancing the vascularization of three-dimensional porous alginate scaffolds by incorporating controlled release basic fibroblast growth factor microspheres. *J Biomed Mater Res A.* 2003; 65: 489–97.
 44. **Mooney DJ, Kaufmann PM, Sano K, et al.** Transplantation of hepatocytes using porous, biodegradable sponges. *Transplant Proc.* 1994; 26: 3425–6.
 45. **Spadaccio C, Chello M, Trombetta M, et al.** Drug releasing systems in cardiovascular tissue engineering. *J Cell Mol Med.* 2009; 13: 422–39.
 46. **Guneyel O, Onur OE, Denizbasi A.** Effects of recombinant human granulocyte colony-stimulating factor (filgrastim) on ECG parameters in neutropenic patients: a single-centre, prospective study. *Clin Drug Investig.* 2009; 29: 551–5.
 47. **Sell SA, McClure MJ, Barnes CP, et al.** Electrospun polydioxanone-elastin blends: potential for bioresorbable vascular grafts. *Biomed Mater.* 2006; 1: 72–80.
 48. **Luong-Van E, Grondahl L, Chua KN, et al.** Controlled release of heparin from poly(epsilon-caprolactone) electrospun fibers. *Biomaterials.* 2006; 27: 2042–50.
 49. **Kim BS, Putnam AJ, Kulik TJ, et al.** Optimizing seeding and culture methods to engineer smooth muscle tissue on biodegradable polymer matrices. *Biotechnol Bioeng.* 1998; 57: 46–54.
 50. **George J, Onodera J, Miyata T.** Biodegradable honeycomb collagen scaffold for dermal tissue engineering. *J Biomed Mater Res A.* 2008; 87: 1103–11.
 51. **Nieponice A, Soletti L, Guan J, et al.** Development of a tissue-engineered vascular graft combining a biodegradable scaffold, muscle-derived stem cells and a rotational vacuum seeding technique. *Biomaterials.* 2008; 29: 825–33.
 52. **Wu X, Rabkin-Aikawa E, Guleserian KJ, et al.** Tissue-engineered microvessels on three-dimensional biodegradable scaffolds using human endothelial progenitor cells. *Am J Physiol Heart Circ Physiol.* 2004; 287: H480–7.
 53. **Onodera N, Tamaki T, Okada Y, et al.** Identification of tissue-specific vasculogenic cells originating from murine uterus. *Histochem Cell Biol.* 2006; 125: 625–35.

54. **He W, Yong T, Teo WE, et al.** Fabrication and endothelialization of collagen-blended biodegradable polymer nanofibers: potential vascular graft for blood vessel tissue engineering. *Tissue Eng.* 2005; 11: 1574–88.
55. **Lafamme MA, Murry CE.** Regenerating the heart. *Nat Biotechnol.* 2005; 23: 845–56.
56. **Menasche P.** Towards the second generation of skeletal myoblasts? *Cardiovasc Res.* 2008; 79: 355–6.
57. **Siepe M, Giraud MN, Liljensten E, et al.** Construction of skeletal myoblast-based polyurethane scaffolds for myocardial repair. *Artif Organs.* 2007; 31: 425–33.
58. **Siepe M, Giraud MN, Pavlovic M, et al.** Myoblast-seeded biodegradable scaffolds to prevent post-myocardial infarction evolution toward heart failure. *J Thorac Cardiovasc Surg.* 2006; 132: 124–31.
59. **Sarkar S, Lee GY, Wong JY, et al.** Development and characterization of a porous micro-patterned scaffold for vascular tissue engineering applications. *Biomaterials.* 2006; 27: 4775–82.
60. **Xu C, Inai R, Kotaki M, et al.** Electrospun nanofiber fabrication as synthetic extracellular matrix and its potential for vascular tissue engineering. *Tissue Eng.* 2004; 10: 1160–8.
61. **Stankus JJ, Soletti L, Fujimoto K, et al.** Fabrication of cell microintegrated blood vessel constructs through electrohydrodynamic atomization. *Biomaterials.* 2007; 28: 2738–46.
62. **Soletti L, Nieponice A, Guan J, et al.** A seeding device for tissue engineered tubular structures. *Biomaterials.* 2006; 27: 4863–70.
63. **Zhang Y, Cheng X, Wang J, et al.** Novel chitosan/collagen scaffold containing transforming growth factor-beta1 DNA for periodontal tissue engineering. *Biochem Biophys Res Commun.* 2006; 344: 362–9.
64. **Huang ZM ZY, Kotaki M, Ramakrishna S.** A review on polymer nanofibers by electrospinning and their applications in nanocomposites. *Compos Sci Technol.* 2003; 63: 2223–53.
65. **Zhang YZ, Venugopal J, Huang ZM, et al.** Characterization of the surface biocompatibility of the electrospun PCL-collagen nanofibers using fibroblasts. *Biomacromolecules.* 2005; 6: 2583–9.
66. **Katti DS, Robinson KW, Ko FK, et al.** Bioresorbable nanofiber-based systems for wound healing and drug delivery: optimization of fabrication parameters. *J Biomed Mater Res B Appl Biomater.* 2004; 70: 286–96.
67. **Kim K, Luu YK, Chang C, et al.** Incorporation and controlled release of a hydrophilic antibiotic using poly(lactide-co-glycolide)-based electrospun nanofibrous scaffolds. *J Control Release.* 2004; 98: 47–56.
68. **Zeng J, Xu X, Chen X, et al.** Biodegradable electrospun fibers for drug delivery. *J Control Release.* 2003; 92: 227–31.
69. **Kenawy el R, Bowlin GL, Mansfield K, et al.** Release of tetracycline hydrochloride from electrospun poly(ethylene-co-vinylacetate), poly(lactic acid), and a blend. *J Control Release.* 2002; 81: 57–64.
70. **Verreck G, Chun I, Rosenblatt J, et al.** Incorporation of drugs in an amorphous state into electrospun nanofibers composed of a water-insoluble, nonbiodegradable polymer. *J Control Release.* 2003; 92: 349–60.
71. **Luu YK, Kim K, Hsiao BS, et al.** Development of a nanostructured DNA delivery scaffold via electrospinning of PLGA and PLA-PEG block copolymers. *J Control Release.* 2003; 89: 341–53.
72. **Spadaccio C, Rainer A, Trombetta M, et al.** Poly-L-lactic acid/hydroxyapatite electrospun nanocomposites induce chondrogenic differentiation of human MSC. *Ann Biomed Eng.* 2009; 37: 1376–89.
73. **Spadaccio C, Rainer A, Chello M, et al.** Drug releasing hybrid scaffold: new avenue in cardiovascular tissue engineering. *Tissue Eng A.* 2008; 14: 691–943.
74. **Guan J, Stankus JJ, Wagner WR.** Biodegradable elastomeric scaffolds with basic fibroblast growth factor release. *J Control Release.* 2007; 120: 70–8.
75. **Ziegler J, Mayr-Wohlfart U, Kessler S, et al.** Adsorption and release properties of growth factors from biodegradable implants. *J Biomed Mater Res.* 2002; 59: 422–8.
76. **Hashi CK, Zhu Y, Yang GY, et al.** Antithrombogenic property of bone marrow mesenchymal stem cells in nanofibrous vascular grafts. *Proc Natl Acad Sci USA.* 2007; 104: 11915–20.
77. **Ghaemi H, Behdinin K, Spence AD.** *In vitro* technique in estimation of passive mechanical properties of bovine heart part I. Experimental techniques and data. *Med Eng Phys.* 2009; 31: 76–82.
78. **Ghaemi H, Behdinin K, Spence AD.** *In vitro* technique in estimation of passive mechanical properties of bovine heart part II. Constitutive relation and finite element analysis. *Med Eng Phys.* 2009; 31: 83–91.
79. **Stroud JD, Baicu CF, Barnes MA, et al.** Viscoelastic properties of pressure overload hypertrophied myocardium: effect of serine protease treatment. *Am J Physiol Heart Circ Physiol.* 2002; 282: H2324–35.
80. **Mainil-Varlet P, Rahn B, Gogolewski S.** Long-term *in vivo* degradation and bone reaction to various polylactides. 1. One-year results. *Biomaterials.* 1997; 18: 257–66.
81. **Guo YH, He JG, Wu JL, et al.** Hepatocyte growth factor and granulocyte colony-stimulating factor form a combined neovascularogenic therapy for ischemic cardiomyopathy. *Cytotherapy.* 2008; 10: 857–67.